Label-free Biosensor Based on Silicon-On-Insulator Concentric Micro-Ring Resonators

Xiaohui Li(1), Ziyang Zhang (2), Shengying Qin(3), Min Qiu (2), Yikai Su (1)
1: State Key Lab of Advanced Optical Communication Systems and Networks, Department of Electronic Engineering, Shanghai Jiao Tong University, 800 Dongchuan Rd, Shanghai 200240, China, yikaisu@sjtu.edu.cn
2: Department of Microelectronics and Applied Physics, Royal Institute of Technology, 164 40 Kista, Sweden
3: Bio-X Life Science Research Center, Shanghai Jiao Tong University, Hao Ran Building, Shanghai 200030, China

Abstract- **We propose a label-free biosensor based on concentric micro-ring resonators in silicon on insulator (SOI). The concentric micro-ring resonators offer another freedom to obtain deeper notches for higher detection sensitivity. The expanded modes also provide larger sensing area. A resonant frequency shift of ~1.37 nm is demonstrated, by numerical simulations, between the situation of using a single strand DNA and a double strand DNA.**

I. INTRODUCTION

Currently the commercialized microarrays usually require labeled molecules detection. However, the labeling step complicates the sample preparation and detection process as the labels can alter the molecules' binding properties and therefore decrease the reliability. Label-free biosensors using direct detection methods attempt to address the stability and reliability issues. Different approaches of direct detection have been reported, such as surface plasmon resonator (SPR) [1], interferometers [2], and resonant cavities [3]. The direct detection of bio-molecular can be used in the monitoring of the molecular dynamics reaction, the quantitative concentration measurements and the determination of affinity contacts.

The silicon-on-insulator (SOI) micro-ring resonator is a promising building-block for ultra-compact and highly integrated photonic circuits. The SOI structure offers high refractive index contrast for nano-scaled photonic circuit fabrication with mostly CMOS-compatible processing techniques.

However, for SOI micro-ring resonators, it is still challenging to achieve deep notches in the transmission spectra for the single-waveguide- single-ring structure. For critical coupling, the resonator intrinsic factor (Qi) and the coupling quality factor with the waveguide (Qe) must be equal. The resonant channel is then completely dropped. Usually, the width of the ring and waveguide and the air gap between them has to be tuned carefully for that purpose. The sensing area is also limited by the small cross-section of the single-mode ring/waveguide. In this paper we propose a two-concentric ring structure to effectively increase the notch depth and increase the sensing area at the same time.

II. CONCERNTRIC RING

A. *Coupled mode theory for concentric ring*

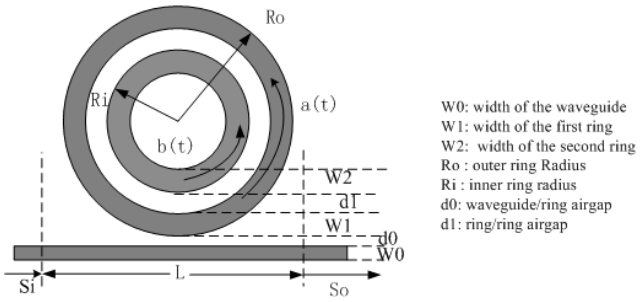

Fig. 1 Schematic of the two concentric ring resonators and a waveguide coupled system.

Fig.1 is the schematic of the device proposed. Here we define the energy of the resonant mode in the outer ring as ***a(t)***, and similarly defined is the inner ring resonant mode ***b(t)***. The coefficients for the waveguide-ring coupling and the ring-ring coupling are denoted as ***k*** and ***u***, respectively. The transfer function can be expressed by [4]

$$T(\omega)=\frac{|S_o|^2}{|S_i|^2}=\left|1-\frac{|k_a^2|[j(\omega-\omega_b)+\frac{1}{\tau_b}]}{[j(\omega-\omega_a)+\frac{1}{\tau_a}][j(\omega-\omega_b)+\frac{1}{\tau_b}]+u^2}\right|^2 \quad (1)$$

where ω_a is the resonant frequency, τ is the photon life time. $1/\tau=1/\tau_e+1/\tau_i$, where $1/\tau_e$ is the decay rate into the waveguide and $1/\tau_i$ is decay rate due to intrinsic loss. The quality factor (Q) is decided by the photon life time, i.e., $Q=\omega_0\tau/2$. The waveguide-ring coupling coefficient and the power decay rate are related by $|\kappa|^2=2/\tau_e$. To simplify the analysis, we only consider the case when the two rings happen to resonate at the same frequency, which can be realized by fine-tuning the free-spectrum-range of the individual rings. For complete drop, the mutual coupling coefficient must satisfy

$$u_m^2=(\frac{1}{\tau_{ae}}-\frac{1}{\tau_{ai}})\frac{1}{\tau_b}=\frac{\omega_0^2}{4Q_b}(\frac{1}{Q_{ae}}-\frac{1}{Q_{ai}}) \quad (2)$$

From Eq.(2), when conventional critical coupling takes place, i.e., when $Q_{ai}=Q_{ae}$, there is no mutual coupling between the rings. When $Q_{ai}\neq Q_{ae}$, the complete drop situation can be achieved with $u^2=u_m^2$.

With the help of the inter-ring coupling, it is possible to attain the improved transmission notch depth and reach new critical coupling. Thus, concentric ring structure opens up

another freedom when designing deep-notch transmission devices.

B. *The Simulation confirmation of mode coupling*

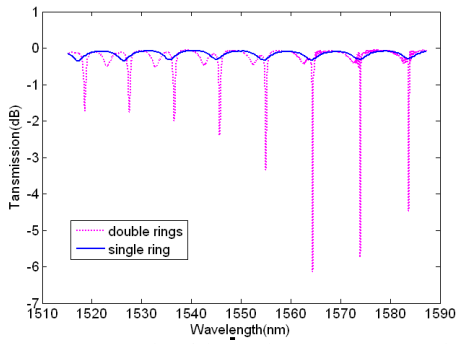

Fig. 2 Transmission results of the single ring resonator and double ring resonators. Solid curve: the 21 μm single ring with 0.1 μm waveguide/ring airgap; dashed curve: the concentric rings with 0.1 μm waveguide/ring and ring/ring airgap

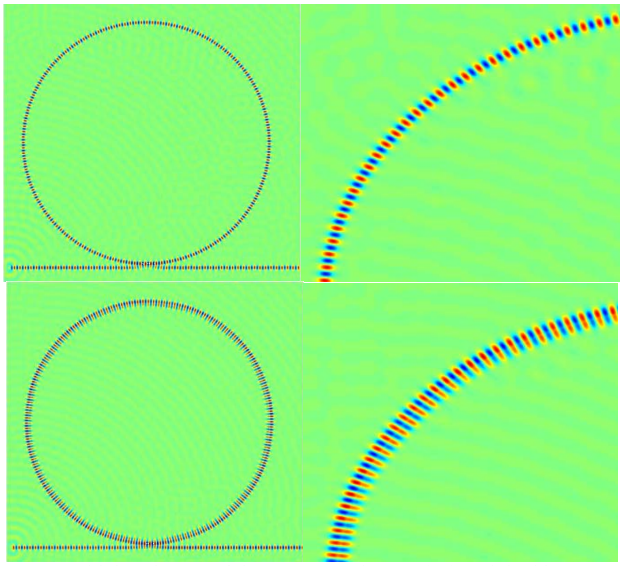

Fig. 3 Field distribution of the 21 μm single ring (up) and double concentric rings (down) at the resonant wavelengths 1564.027 and 1564.394nm, respectively, with the same structural parameters as those in Fig. 2. The left ones are the whole view and the right ones are zoom-in pictures.

We perform two-dimensional finite difference time domain (2D FDTD) simulations to study the transmission spectra of the concentric ring resonators. Fig.2 shows the improvement of the transmission notches with one more ring placed concentrically in the single–ring-single-waveguide system. The notch enhancement at 1564 nm is about 6 dB.

Fig.3 indicates the field distributions. It is clearly seen that the light is almost evenly distributed in the double ring structure, offering larger sensing area.

C. *The device fabrication and results*

We use commercial SOI wafers for the device fabrication. The top silicon layer is 250-nm thick and the silica buffer layer is 3 μm. The device pattern is firstly defined in electron beam lithography (Raith 150, 25kV) and then transferred to the silicon layer by reactive ion etching. The waveguide width starts with 10 μm and gradually tapers down to 480 nm. The ring cross-section is 500 nm (wide) by 250 nm (thick). The width of the air gap between the ring and waveguide is ~110 nm to ensure good coupling with the waveguide.

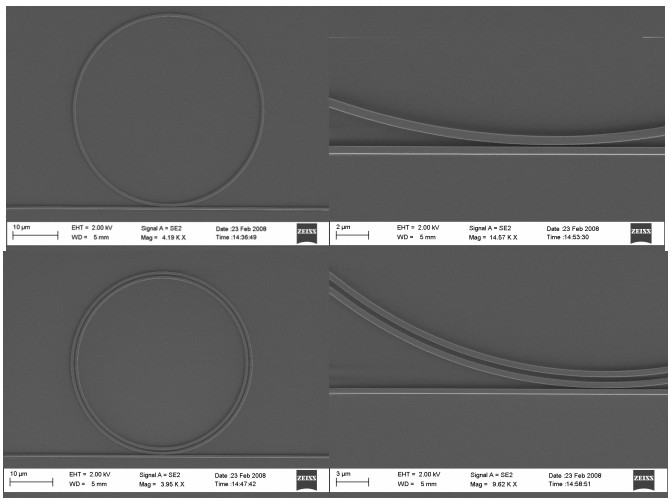

Fig. 4 SEM photos of (up) a single 21-μm-radius ring side coupled to a waveguide and (down) concentric double-ring structure with outer ring radius 21 μm, inner ring radius 20.02 μm, and airgap width 480 nm between the rings. The left ones are the whole view and the right ones are zoom-in pictures.

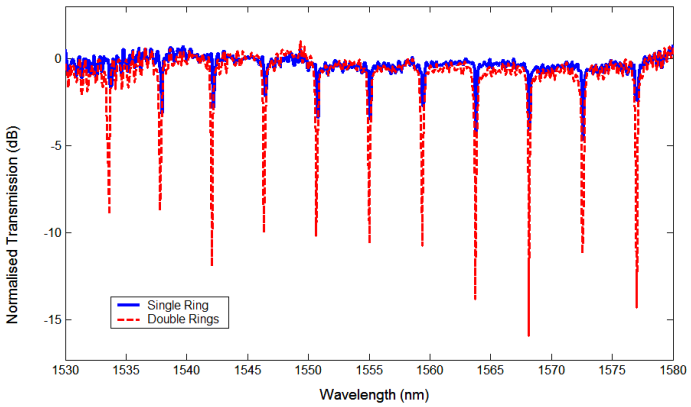

Fig. 5 Transmission measurement results: the full spectrum scans for the single ring (solid curve) and double ring (dashed curve) structures shown in Fig.4.

The SEM photos of the 21-μm-radius-outer ring structure are shown in Fig. 4. The transmission measurement results are shown in Fig. 5. Around 1568.14 nm, the notch depth improves about 15 dB. The intrinsic Q is estimated to be ~ 5.1×10^4.

III. LABLE-FREE DETECTION USING CONCENTRIC RINGS

For label-free biosensors based on the optical resonators, the sensing of the DNA hybridization is realized by the detection of the resonance shift of the micro-rings. This is based on the fact that the effective refractive index of the waveguide changes after the DNA hybridization, i.e., when single strand DNA (ssDNA) becomes double strands DNA (dsDNA). The magnitude of the resonant frequency shift

depends on factors such as the bio-layer thickness, the changes of the effective refractive index of the bond targets, and etc.

We assume that the ssDNA is initially functionalized on top of the air gap in the ring resonators as the detection probe. When complementary DNA strands appear in the detection process, they will hybridize with the functionalized capture probes forming dsDNA.

When the concentric ring resonators are used to detect the DNA strands, the detecting areas are enlarged due to the expanded field distribution. The refractive indexes of ssDNA and dsDNA layers are around 1.456 and 1.53, respectively [5]. To model this, we perform 2D FDTD simulations to study the transmission of different conditions. The transmission spectra (Fig .6) show the resonant frequency shift of the double ring resonators detector. In Fig.6 (b) the resonant shift around 1560 nm is 1.37nm.

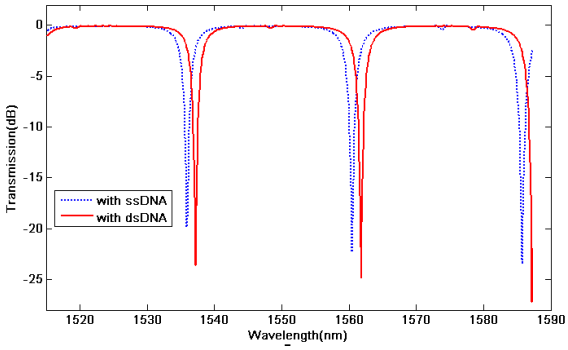

(a)

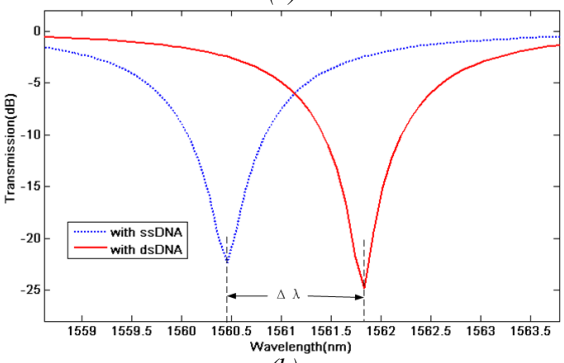

(b)

Fig. 6 (a) Simulation results of transmission spectra before (dashed curve) and after (solid curve) detection in double ring resonators device with outer ring radius 5 μm, width of the waveguide and rings 0.5μm, ring/ring airgap 0.3μm,waveguide/ring airgap0.1μm .(b) is the zoom-in picture of the transmission of (a) around the second notch.

IV. CONSLUSION

In this work we have proposed a method to detect the DNA hybridization. We analyze, fabricate and demonstrate concentric micro-ring resonators in the SOI structure for enhanced transmission notches. FDTD simulations confirm the enlarged modal area for concentric ring resonators. When the complementary strand DNA attaches with the probe DNA, the refractive index of the resonators changes and causes a significant resonant frequency shift.

ACKNOWLEDGMENT

This work was supported by the NSFC (60777040), Shanghai Rising Star Program Phase II (07QH14008), Swedish Foundation for Strategic Research (SSF), and the Swedish Research Council (VR).

REFERENCES

[1] P.P.P. Debackere, et al, "Surface Plasmon Interferometer in silicon-on-Insulator: novel concept for an integrated biosensor," Opt. Express 14, 7063-7072 (2006).

[2] A.Ymeti, et al, "Fast, ultrasensitive virus detection using a Young interferometer sensor," Nano.Lett..7, 394-397 (2007).

[3] A.Ksendzov,Y.Lin, "Integrated Optics Ring-resonator Sensors for Protein Detection" Opt.Lett.30, 3344-3346 (2005).

[4] Z. Zhang et al, "Resonance-splitting and enhanced notch depth in SOI ring resonators with mutual mode coupling," Opt. Express..16, 4621-4630 (2008).

[5] S. Elhadj, et al, "Optical Properties of an Immobilized DNA Monolayer from 255 to 700 nm," Langmuir 20, 5539-5543 (2004).